# *S*-Wave Spin-Triplet Order in Superconductors without Inversion Symmetry: $Li_2Pd_3B$ and $Li_2Pt_3B$

H. Q. Yuan,[1,*] D. F. Agterberg,[2] N. Hayashi,[3] P. Badica,[4,5] D. Vandervelde,[1] K. Togano,[6] M. Sigrist,[3] and M. B. Salamon[1]

[1]*Department of Physics, University of Illinois at Urbana and Champaign, 1110 West Green Street, Urbana, Illinois 61801, USA*

[2]*Department of Physics, University of Wisconsin—Milwaukee, Milwaukee, Wisconsin 53201, USA*

[3]*Theoretische Physik, ETH-Zürich, CH-8093 Zürich, Switzerland*

[4]*Institute for Materials Research, Tohoku University, 2-1-1 Katahira, Aoba-ku, Sendai 980-8577, Japan*

[5]*National Institute of Materials Physics, P.O. Box MG-7, Bucharest 077125, Romania*

[6]*National Institute for Materials Science, 1-2-1 Sengen, Tsukuba 305-0047, Japan*

(Received 20 December 2005; published 7 July 2006)

We investigate the order parameter of noncentrosymmetric superconductors $Li_2Pd_3B$ and $Li_2Pt_3B$ via the behavior of the penetration depth $\lambda(T)$. The low-temperature penetration depth shows BCS-like behavior in $Li_2Pd_3B$, while in $Li_2Pt_3B$ it follows a linear temperature dependence. We propose that broken inversion symmetry and the accompanying antisymmetric spin-orbit coupling, which admix spin-singlet and spin-triplet pairing, are responsible for this behavior. The triplet contribution is weak in $Li_2Pd_3B$, leading to a wholly open but anisotropic gap. The significantly larger spin-orbit coupling in $Li_2Pt_3B$ allows the spin-triplet component to be larger in $Li_2Pt_3B$, producing line nodes in the energy gap as evidenced by the linear temperature dependence of $\lambda(T)$. The experimental data are in quantitative agreement with theory.

DOI: 10.1103/PhysRevLett.97.017006 PACS numbers: 74.20.Rp, 71.70.Ej, 74.70.Dd

The crystal structure of most superconducting materials investigated to date includes a center of inversion. The Pauli principle and parity conservation then dictate that superconducting pairing states with even parity are necessarily spin singlet, while those with odd parity must be spin triplet [1]. In materials that lack inversion symmetry, the tie between spatial symmetry and the Cooper-pair spin may be broken [2–7]. The absence of inversion symmetry along with parity-violating antisymmetric spin-orbit coupling (ASOC) allows admixture of spin-singlet and spin-triplet components. Unconventional behavior, including zeroes in the superconducting gap function, is then possible, even if the pair wave function exhibits the full spatial symmetry of the crystal.

In this Letter we report the dramatically different electrodynamic behavior of two newly discovered noncentrosymmetric superconductors $Li_2Pd_3B$ and $Li_2Pt_3B$ [8,9]. The penetration depth $\lambda(T)$ in the former material has the expected exponential temperature dependence of a fully gapped superconductor, while the latter exhibits a linear temperature dependence over the range $0.05 \leq T/T_c \leq 0.3$. Inasmuch as the main difference between these two compounds is the larger spin-orbit coupling strength for Pt $[(Z_{Pt}/Z_{Pd})^2 = 2.9$: $Z$ is the atomic number], we argue that the unconventional behavior is evidence for admixed singlet and triplet order as a consequence of ASOC. Indeed, we show quantitative agreement between the experimental data of $\lambda(T)$ and the theoretical calculations for mixed singlet and triplet states based on ASOC.

Parity-broken superconductivity (SC) was previously discussed in the context of surface superconductors [5] and for dirty bulk materials [6]. Recently, the discovery of SC in the magnetic compounds $CePt_3Si$ [10], UIr [11], and $CeRhSi_3$ [12] (under pressure) has attracted extensive interest in studying SC without inversion symmetry. Unfortunately, in these correlated-electron systems the nature of superconductivity is complicated by its coexistence with magnetism, therefore severely restricting the study of parity-broken SC.

$Li_2Pd_3B$ and $Li_2Pt_3B$ crystallize in a perovskitelike cubic structure composed of distorted octahedral units of $BPd_6$ and $BPt_6$ [13]. Unlike $CePt_3Si$, $CeRhSi_3$, and UIr, these materials show no evidence of magnetic order or strong correlated-electron effects [8,9,14–16] that could lead to unconventional superconducting behavior. Further, the increased spin-orbit coupling in Pt leads to much larger band splitting in $Li_2Pt_3B$ than in $Li_2Pd_3B$ [17], allowing us to study the dependence of superconductivity on the ASOC strength. Therefore, we argue that $Li_2Pd_3B$ and $Li_2Pt_3B$ provide a *model system* in which to study SC without inversion symmetry.

Polycrystalline samples of $Li_2Pd_3B$ and $Li_2Pt_3B$ were prepared by arc melting [8,9]. Powder x-ray diffraction and metallography identify them as being single phase. The sharp superconducting transitions with a width less than 10% of $T_c$ observed in either bulk magnetization $M(T)$ (see, e.g., the inset of Fig. 1), penetration depth $\lambda(T)$, or electrical resistivity $\rho(T)$ (not shown) indicate good sample homogeneity. The mean free path [18], estimated from the rf resistivity $\rho$ at $T_c$, coherence length $\xi$, and specific heat coefficient $\gamma$ [15] ($\rho = 20\ \mu\Omega\,\mathrm{cm}$, $\xi = 9.5$ nm, $\gamma = 9\ \mathrm{mJ/molK^2}$ for $Li_2Pd_3B$ and $\rho = 28\ \mu\Omega\,\mathrm{cm}$, $\xi = 14.5$ nm, $\gamma = 7\ \mathrm{mJ/molK^2}$ for $Li_2Pt_3B$), is 24 nm for $Li_2Pd_3B$ and 42 nm for $Li_2Pt_3B$, a few times larger than the corresponding coherence length, indicating clean samples. Precise measurements of penetration depth

 

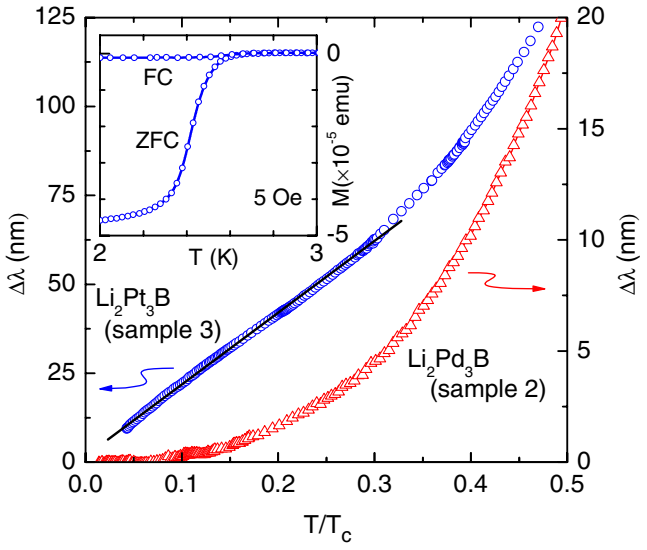


FIG. 1 (color online). Temperature dependence of the penetration depth $\triangle\lambda(T)$ for $Li_2Pd_3B$ (sample 2) and $Li_2Pt_3B$ (sample 3), showing distinct low-temperature behavior [20]. The inset shows the magnetization $M(T)$ for $Li_2Pt_3B$ (sample 3) measured in zero field cooling (ZFC) and field cooling (FC) in a magnetic field of 5 Oe. The values of $T_c$ [$T_c = 6.7$ K for $Li_2Pd_3B$ (sample 2) and $T_c = 2.43$ K for $Li_2Pt_3B$ (sample 3)] were determined from the midpoints of magnetization drop at $T_c$.

$\Delta\lambda(T)$ were performed utilizing a tunnel-diode based, self-inductive technique at 21 MHz down to 90 mK in a dilution refrigerator. The change in penetration depth $\Delta\lambda(T)$ is proportional to the resonant frequency shift $\Delta f(T)$, i.e., $\Delta\lambda(T) = G\Delta f(T)$, where the factor $G$ is determined by sample and coil geometries [19]. Because of the uneven sample surface, the uncertainty of the $G$ factor can be up to 15%. In this Letter, $\Delta\lambda(T)$ is extrapolated to zero at $T = 0$, i.e., $\Delta\lambda(T) = \lambda(T) - \lambda_0$. The values of zero temperature penetration depth $\lambda_0$ ($\lambda_0 = 190$ nm for $Li_2Pd_3B$ and $\lambda_0 = 364$ nm for $Li_2Pt_3B$) are taken from Ref. [9], determined from the magnetic critical field measurements. The difference of $\lambda_0$ in the two compounds might result from their distinct Fermi surfaces due in part to the spin-orbit coupling [17]. The magnetization $M(T, H)$ was measured using a commercial SQUID magnetometer (MPMS, Quantum Design).

In Fig. 1 the penetration depth change $\Delta\lambda(T)$ is shown for $Li_2Pd_3B$ and $Li_2Pt_3B$, respectively. The nearly $T$ independence of $\lambda(T)$ at low temperatures for the Pd compound is characteristic of fully gapped behavior, consistent with NMR experiments [14] and specific heat measurements [15]. However, the penetration depth $\lambda(T)$ of $Li_2Pt_3B$ follows a linear temperature dependence [20]. Such a $T$-linear behavior of $\lambda(T)$ can be theoretically interpreted by (a) phase fluctuations among Josephson-coupled grains [21] and (b) line nodes in the superconducting energy gap. The former one can be ruled out in this context. The importance of phase fluctuations depends inversely on grain size, which is large ($> 100$ $\mu$m) in both the Pt and Pd samples [8]. If phase fluctuations dominate, the Pd sample, with comparable normal-state resistivity and grain size, should also show a strong linear temperature dependence. Further, the transition temperature $T_c$ is strongly dependent on the normal-state resistivity in the phase-fluctuation regime. We find that the $T_c$ varies by less than 10% among samples that have normal-state resistivities that differ by a factor of 3 or more. Finally, we have reanalyzed the specific heat of $Li_2Pt_3B$ reported in Ref. [15] and find that $C_{el}/T \sim T$ is a much better representation of those data at low temperature than is an exponential dependence, further supporting the existence of line nodes.

Before describing our model, we explore possible non-$s$-wave states that might exhibit line nodes in $Li_2Pt_3B$. The weak-coupling theory of SC, justified by the low $T_c$, permits only the following three states: (i) $\Delta_+(\mathbf{k}) \simeq \Delta_-(\mathbf{k}) = (k_x^2 - k_y^2)(k_y^2 - k_z^2)(k_z^2 - k_x^2)$; (ii) $\Delta_+(\mathbf{k}, z) \simeq \Delta_-(\mathbf{k}, z) = e^{iqz}k_z[k_y(k_y^2 - k_z^2) + ik_x(k_z^2 - k_x^2)]$; (iii) $\Delta_+(\mathbf{k}, z) \simeq \Delta_-(\mathbf{k}, z) = e^{iqz}k_z(k_x + ik_y)$. In the latter two cases, broken parity and time reversal symmetries combine to destabilize the spatially uniform state, giving rise to the spatial dependence in the gap functions. The former two states are unlikely in any theory that is based on local interactions (like the single band Hubbard model). Since the above three states are not $s$-wave pairing states, and (as argued below) $Li_2Pd_3B$ appears to be an $s$ wave, a phase transition in the pairing state of $Li_2(Pd_{1-x}Pt_x)_3B$ with varying $x$ would have to occur for any of these states to exist in $Li_2Pt_3B$. Furthermore, these states should be extremely sensitive to impurities and $T_c$ should be strongly suppressed when $x$ is varied from 1. These are in contrast with the experimentally observed smooth evolution of $T_c$ with $x$ [9]. Given these arguments against unconventional superconductivity, we attribute the dramatic difference between these two compounds to the variation of ASOC.

When parity symmetry is violated, the ASOC that breaks the spin degeneracy of each band takes the form $\alpha\mathbf{g}(\mathbf{k}) \cdot \mathbf{S}(\mathbf{k})/\hbar$, where $\alpha$ denotes the spin-orbit coupling strength, $\mathbf{S}(\mathbf{k})$ is the spin of an electron with momentum $\hbar\mathbf{k}$, and $\mathbf{g}(\mathbf{k})$ is a dimensionless vector [$\mathbf{g}(-\mathbf{k}) = -\mathbf{g}(\mathbf{k})$ to preserve time reversal symmetry]. This ASOC leads to an energy splitting of the originally degenerate spin states and results in spin eigenstates that are polarized parallel or antiparallel to $\mathbf{g}(\mathbf{k})$. The ASOC plays a crucial role in the determination of the superconducting state. The key point is that if a spin-triplet contribution to the superconducting gap function is to emerge, its characteristic $d$ vector $\mathbf{d}(\mathbf{k})$ must be parallel to $\mathbf{g}(\mathbf{k})$ (provided that the ASOC is sufficiently large) [3,4]. This leads to two gap functions $\Delta_\pm(\mathbf{k}) = \psi \pm t|\mathbf{g}(\mathbf{k})|$, where each gap is defined on one of the two bands formed by the degeneracy lifting of the ASOC; $\psi$ and $t$ are the singlet and triplet order parameters, respectively. For a range of values of $\nu = \psi/t$, $\Delta_-(\mathbf{k})$ can change sign and nodes may exist in the superconducting gap.

Recent band structure calculations for these compounds [17] provide information about $|\mathbf{g}(\mathbf{k})|$. These results indicate that $\alpha$ is a large energy scale relative to the bandwidth and that $|\mathbf{g}(\mathbf{k})|$ is highly anisotropic. To capture these results in a model, we take $\mathbf{g}(\mathbf{k}) = a_1\mathbf{k} - a_2[\hat{\mathbf{x}}k_x(k_y^2 + k_z^2) + \hat{\mathbf{y}}k_y(k_z^2 + k_x^2) + \hat{\mathbf{z}}k_z(k_x^2 + k_y^2)]$, with $a_2/a_1 = 3/2$, $\mathbf{k}$ a unit vector, and the spherical average of $|\mathbf{g}(\mathbf{k})|^2$ equal to unity. This form of $|\mathbf{g}(\mathbf{k})|$ is the simplest that is consistent with cubic symmetry and allows for anisotropy on a model, spherical Fermi surface.

We compute the penetration depth (the superfluid density) on the basis of the formula described in [22]. These fits provide estimates for $\nu$ (defined at $T \to T_c$) and $\delta$, the ratio of the relative density of states between the spin-orbit-split bands. The resulting fits are shown in Figs. 2(a) and 3(a), respectively. $Li_2Pd_3B$ is nearly a pure spin-singlet state, with a large value of $\nu \simeq 4$. We note that the preliminary fit of two-band model in $Li_2Pd_3B$ with a fraction of 4% from the small energy gap [20] treated data only for $T < 0.3T_c$, while the present analysis covers the whole temperature range. As argued above, $Li_2Pt_3B$ clearly evidences line nodes, meaning that $\Delta_-(\mathbf{k})$ changes sign for a range of wave vectors. The best fit for $Li_2Pt_3B$ has $\nu = 0.6$ and $\delta = 0.3$, indicating that the spin-triplet component is dominant. We expect $\delta$ to be proportional to the strength $\alpha$ of the ASOC, which in turn varies as the square of the atomic number, as above. The obtained value of $\delta(\mathrm{Pt})/\delta(\mathrm{Pd}) = 0.3/0.1 = 3$ is consistent with the expectations. In the insets to Figs. 2(a) and 3(a) we show polar plots of $\Delta_-(\mathbf{k})$ for the two compounds; for $Li_2Pt_3B$, the existence of line nodes appears in the form of circular bands. For $Li_2Pd_3B$, both $\Delta_+(\mathbf{k})$ and $\Delta_-(\mathbf{k})$ are nonzero, but anisotropic, over the entire Fermi surface. It is noted that the gap functions $\Delta_+(\mathbf{k})$ and $\Delta_-(\mathbf{k})$ possess cubic symmetry [see

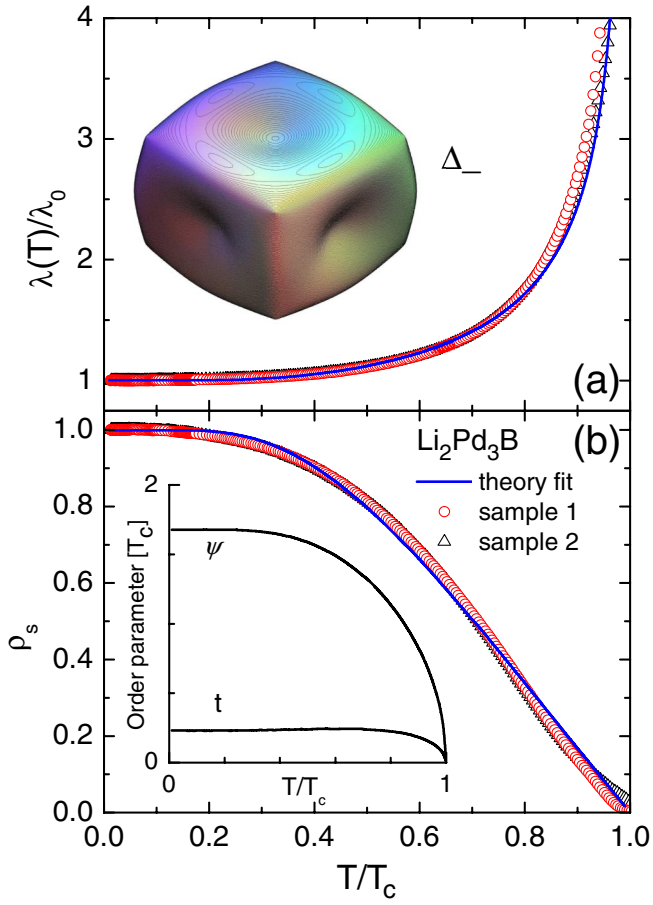


FIG. 2 (color online). The temperature dependence of (a) the normalized penetration depth $\lambda(T)/\lambda_0$ and (b) the corresponding superfluid density $\rho_s(T)$ for $Li_2Pd_3B$, in which $T_c = 7$ K, $G = 0.42$ nm/Hz for sample 1 and $T_c = 6.7$ K, $G = 0.63$ nm/Hz for sample 2. The symbols, as described in the figure, represent the experimental data, and the solid line is a theoretical fit with parameters $\delta = 0.1$ and $\nu = 4$. The insets in the upper panel and the lower panel show a 3D polar plot of the gap function $\Delta_-(\mathbf{k})$ and the temperature dependence of the order parameter components $\psi$ (spin singlet) and $t$ (spin triplet), respectively.

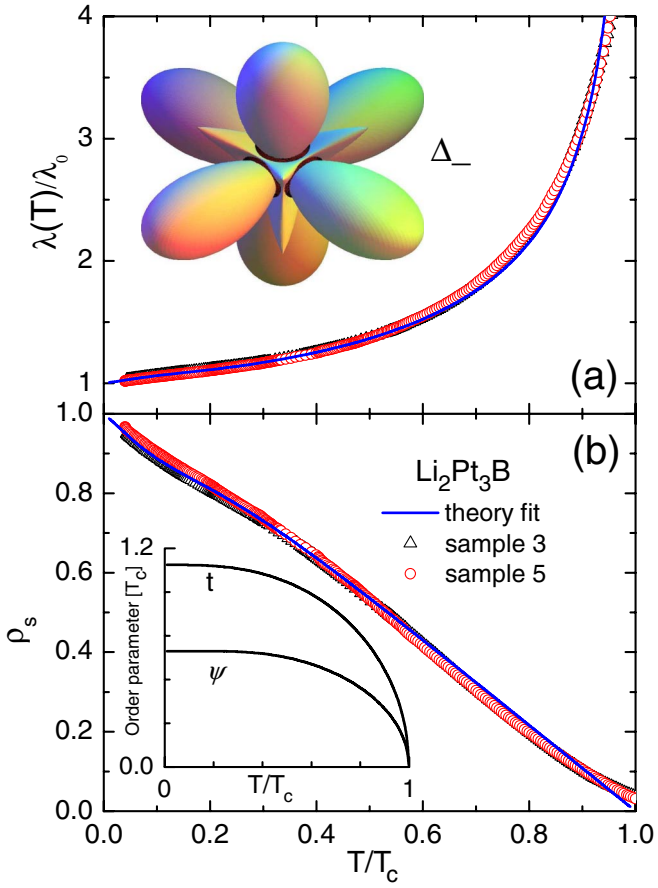


FIG. 3 (color online). The temperature dependence of (a) the normalized penetration depth $\lambda(T)/\lambda_0$ and (b) the corresponding superfluid density $\rho_s(T)$ for $Li_2Pt_3B$, in which $T_c = 2.43$ K, $G = 1$ nm/Hz for sample 3 and $T_c = 2.3$ K, $G = 0.41$ nm/Hz for sample 5. The fitting parameters are $\delta = 0.3$ and $\nu = 0.6$. In $Li_2Pt_3B$, the spin-triplet component $t$ is the dominant order parameter [inset of panel (b)]. In order to clearly show the line nodes, a small constant is added to the gap function $\Delta_-(\mathbf{k})$ [inset of panel (a)]. Six circlelike line nodes can be seen along the large lobes as marked by the dark lines. $\Delta_-(\mathbf{k})$ changes sign from the large lobes ( + ) to the small lobes (−) in the 3D polar plot.

the insets of Figs. 2(a) and 3(a)] and the pairing states break only gauge invariance symmetry, i.e., an $s$-wave orbital symmetry for both $Li_2Pd_3B$ and $Li_2Pt_3B$. However, $\Delta_-(\mathbf{k})$ exhibits a sign change in $Li_2Pt_3B$ indicated by dark circles in Fig. 3(a). Figures 2(b) and 3(b) present the superfluid density $\rho_s(T)$ obtained from the penetration depth $[\rho_s(T) = \lambda_0^2/\lambda^2(T)]$, along with calculated curves. The agreement is satisfactory. One notes that the weak tail in the experimental $\rho_s(T)$ as $T \rightarrow T_c$ is mainly due to the influence of rf skin depth upon approaching $T_c$. The insets of Figs. 2(b) and 3(b) show the calculated temperature dependences of the order parameters $\psi$ and $t$. Obviously, the spin-singlet component is dominant in the order parameter of $Li_2Pd_3B$, but it is not the case in $Li_2Pt_3B$. For the latter compound, the spin-triplet component $t$ is sufficiently large to give rise to the existence of line nodes in the superconducting energy gap. The existence of a spin-triplet state may be stabilized by the ''interparity'' coupling (termed $e_m$ in Ref. [4]) between singlet and triplet channels as allowed by broken inversion symmetry. This interaction can arise from $e$l-ph (and $e$l-$e$l) coupling and may dominate in $Li_2Pt_3B$ because of the large ASOC [17]. We note that while our model (spherical Fermi surface and isotropic spin-singlet gap) predicts that spin-triplet component is larger than the spin-singlet component, this need not be the case in reality. In particular, if the spin-singlet gap is anisotropic, then the Fermi surface average of the magnitude of the spin-triplet component required to produce line nodes can be significantly decreased.

In addition to the profound effect on the pairing state in $Li_2Pt_3B$, broken parity symmetry has other nontrivial consequences. For example, the cubic symmetry allows for a novel contribution to the Ginzburg-Landau (GL) free energy density of the form $\varepsilon \mathbf{B} \cdot \mathbf{j}_{so}$, where $\mathbf{j}_{so}$ is the supercurrent as defined in the usual GL theory and $\varepsilon$ is a constant. As a consequence, the condensate wave function will not be spatially uniform along the direction of the applied magnetic field as it usually is. Near the upper critical field, it will develop a finite center of mass momentum that is parallel to the applied field [23]. This helical structure of the order parameter is similar to that of a Fulde-Ferrell-Larkin-Ovchinnikov (FFLO) superconductor [24,25]. However, in contrast to the FFLO phase, a nonzero center of mass momentum exists at all temperatures. In the vortex state, this coupling term causes the magnetization to develop a transverse component that is parallel to the supercurrent. This may be observable through small angle neutron scattering experiments.

In summary, our observations have demonstrated that superconductors lacking inversion symmetry exhibit qualitatively distinct properties from those with an inversion center. The existence of unconventional properties (e.g., line nodes) for an $s$-wave–type superconductor found in $Li_2Pt_3B$ provides an alternative way to study unconventional SC, especially that arising from phonon pairing mechanism. Indeed, the absence of parity symmetry coupled with strong spin-orbit coupling, which results in an admixture of spin-singlet and spin-triplet pairing, requires a complete reconceptualization of Cooper pairs and the nature of the superconducting state.

We thank P. Frigeri, R. Kaur, I. Milat, and H. Takeya for useful discussions. This work is supported by the National Science Foundation under Grants No. NSF-EIA0121568 and No. NSF-DMR0318665, the Department of Energy under Grant No. DEFG02-91ER45439, the Swiss National Science Foundation and Petroleum Research Funds. We also acknowledge support from ICAM (H. Q. Y.), the 2003-PFRA program of Japan Society for the Promotion of Science (N. H.), and the Romanian CEEX 27/2005 program (P. B.).

*Electronic address: yuan@mrl.uiuc.edu

[1] See, e.g., T. Moriya and K. Ueda, Rep. Prog. Phys. **66**, 1299 (2003); A. P. Mackenzie and Y. Maeno, Rev. Mod. Phys. **75**, 657 (2003).
[2] L. P. Gor'kov and E. I. Rashba, Phys. Rev. Lett. **87**, 037004 (2001).
[3] P. A. Frigeri *et al.*, Phys. Rev. Lett. **92**, 097001 (2004).
[4] P. A. Frigeri *et al.*, cond-mat/0505108.
[5] V. M. Edel'stein, Sov. Phys. JETP **68**, 1244 (1989).
[6] L. S. Levitov, Yu. V. Nazarov, and G. M. Eliashberg, JETP Lett. **41**, 445 (1985).
[7] K. V. Samokhin, E. S. Zijlstra, and S. K. Bose, Phys. Rev. B **69**, 094514 (2004); **70**, 069902(E) (2004).
[8] K. Togano *et al.*, Phys. Rev. Lett. **93**, 247004 (2004).
[9] P. Badica, T. Kondo, and K. Togano, J. Phys. Soc. Jpn. **74**, 1014 (2005).
[10] E. Bauer *et al.*, Phys. Rev. Lett. **92**, 027003 (2004).
[11] T. Akazawa *et al.*, J. Phys. Condens. Matter **16**, L29 (2004).
[12] N. Kimura *et al.*, Phys. Rev. Lett. **95**, 247004 (2005).
[13] U. Eibenstein and W. Jung, J. Solid State Chem. **133**, 21 (1997).
[14] M. Nishiyama, Y. Inada, and G. Q. Zheng, Phys. Rev. B **71**, 220505(R) (2005).
[15] H. Takeya *et al.*, Phys. Rev. B **72**, 104506 (2005).
[16] T. Yokoya *et al.*, Phys. Rev. B **71**, 092507 (2005).
[17] K.-W. Lee and W. E. Pickett, Phys. Rev. B **72**, 174505 (2005).
[18] The mean free path can be written as $l_{tr} = (\frac{\xi^{-2} - 1.6\times10^{12}\rho_{\Omega\,cm}\gamma T_c}{1.8\times10^{24}(\rho_{\Omega\,cm}\gamma T_c)^2})^{0.5}$ by canceling the Fermi-velocity-related term in the expressions of the Ginzburg-Landau coherence length and the mean free path [see, e.g., the appendix in T. P. Orlando *et al.*, Phys. Rev. B **19**, 4545 (1979)].
[19] E. E. M. Chia *et al.*, Phys. Rev. B **67**, 014527 (2003).
[20] H. Q. Yuan *et al.*, cond-mat/0506771.
[21] C. Ebner and D. Stroud, Phys. Rev. B **28**, 5053 (1983).
[22] N. Hayashi *et al.*, Phys. Rev. B **73**, 024504 (2006).
[23] R. P. Kaur, D. F. Agterberg, and M. Sigrist, Phys. Rev. Lett. **94**, 137002 (2005).
[24] P. Fulde and R. A. Ferrell, Phys. Rev. **135**, A550 (1964).
[25] A. I. Larkin and Y. N. Ovchinnikov, Sov. Phys. JETP **20**, 762 (1965).